Model-Based Adaptive Filtering of Dielectric Elastomer Loudspeakers

EMIL GARNELL,

(emil.garnell@gmail.com)

OLIVIER DOARÉ, *AES Associate Member* **AND CORINNE ROUBY**

(olivier.doare@ensta-paris.fr)   (corinne.rouby@ensta-paris.fr)

IMSIA, CNRS, ENSTA Paris, EDF, CEA, Institut Polytechnique de Paris, Paris, France

Dielectric elastomers are soft actuators that can reach deformations by more than 500% when a high voltage is applied. They have been considered for use as loudspeakers because of their quick response. One of their limitations is an inhomogeneous frequency response, due to the modal behavior of the membrane. In this study, we set up a sensor-free adaptive filtering strategy that relies on a finite element model of the loudspeaker, to improve the frequency response.

0 INTRODUCTION

Dielectric elastomers (DEs) are soft active materials that have first been studied about 20 years ago. They are made of a thin layer of elastomer coated on its two sides by compliant electrodes to form a deformable capacitor [1]. When a high voltage (typically 2,000 V) is applied between the electrodes, an electrostatic pressure squeezes the membrane, which thins down and, because of the incompressibility of the elastomer, increases in area. Increases in area by up to more than 480% can be reached [2] without any instability. Because of their high energy density and quick response, DEs have been considered for a wide range of applications, including artificial muscles, soft robotics, pumps, etc.

As DE membranes are very thin and lightweight and respond quickly to an electrical stimuli, they are good candidates for making cheap and lightweight loudspeakers, so research groups have started investigating audio applications of DEs [3, 4], and patents were deposited [5, 6]. Many studies on the sound radiation properties of DE loudspeakers in different configurations followed [7–10]. The sole mechanism of increase of the membrane area when actuated is not able to radiate sound, as it generates very little volume change (except if many layers of DE are stacked [10]). It is therefore necessary to bias the system to convert the increase in area to an increase in volume. That is why one of the most studied designs of DE loudspeakers consists of a membrane inflated over a closed cavity, as shown in Fig. 1. This design has been investigated ex-

perimentally [11], and a few numerical studies analyzed the membrane dynamics [12, 13]. We recently developed a model that takes into account the strong coupling between the electrostatics, the membrane dynamics, and acoustics. The numerical simulations showed good agreement with our experiments [14, 15].

One of the limitations of DE loudspeakers is their acoustic frequency response, which exhibits many sharp peaks and drops because of the modal behavior of the membrane. Two paths can be taken to address this problem: First, adding damping into the system may help flattening the frequency response [16], and second, the signal can be equalized before being sent to the loudspeaker [17, 18]. Indeed, by filtering the music signal, the frequency response of the loudspeaker can be tuned in a very flexible way to reach various objectives depending on the context. The most common goal is to flatten the frequency response [19] to obtain a neutral system that reproduces the original signal. This approach is getting quite generalized nowadays for standard electrodynamic loudspeakers as powerful digital signal processors become inexpensive [20]. Equalization should be seen as a good complement to physical optimization, once the system cannot be improved any further by adjusting the geometry of the transducers [21] or adding damping for example.

Mainly two types of equalization filters are used: finite impulse response (FIR) and infinite impulse response (IIR) filters. FIR filters are always stable, can be easily designed by frequency-domain deconvolution [17], and allow both magnitude and phase equalization [22]. This method may
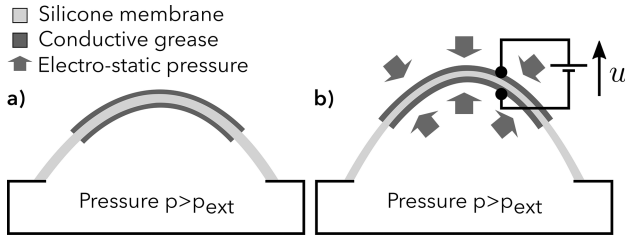
Fig. 1. Principle of inflated dielectric elastomer loudspeakers. When a high voltage is applied, the membrane is squeezed by the electrostatic pressure, and as it is incompressible, it increases in area. The bias pressure then pushes it outward, increasing the volume of the inflated membrane. By repeating this process, an acoustic volume source is obtained [3]. a) Voltage off. b) Voltage on.

Fig. 2. Picture of the prototype during acoustical measurement in an anechoic chamber.

induce preringing, which is more noticeable than postringing [22, 23]. However, Norcross et al. [24] proposed a modified frequency-domain deconvolution technique to design inverse FIR filters with minimum phase, which ensures that there is no preringing. The main drawback of equalization with FIR filters is that long impulse responses are often needed, especially when working on low frequencies [22]. IIR filters are shorter and often computationally more efficient, but their design is more difficult as they may be unstable.

Equalization has been investigated for DE loudspeaker arrays by Klug et al. [25], but this approach is immediately confronted to an inherent limit of DE actuators: They are made of elastomeric materials whose properties tend to change over time because of material aging, temperature variations, and, in the case of the inflated membrane, inflation pressure fluctuations. This implies that compensation filters must adapt to follow the evolution of the system. To this end, the filter adaptation has to rely on some measurements. In the present study, we propose to use impedance measurements only so that no added sensor is needed. A multiphysics finite element model of the loudspeaker is then used to design and adapt the inverse filter.

The article is organized as follows: first the studied inflated DE loudspeaker is described, the model is quickly introduced, as well as the numerical method to solve for the acoustic frequency response using a finite element code. The adaptive filtering strategy is then presented in Sec. 2, and its efficiency is assessed in Sec. 3 by measurements on a prototype.

1 DESCRIPTION OF THE STUDIED SYSTEM

In this section, the studied device and the modeling procedure are presented, and the model is validated by experimental investigations. The need for an accurate model of the sound radiation of the DE loudspeaker is justified in detail in Sec. 2, in which the adaption algorithm is described.

1.1 Description of the Experimental Setup

An inflated dielectric elastomer loudspeaker has been manufactured, using a 50-μm-thick silicone membrane bi-

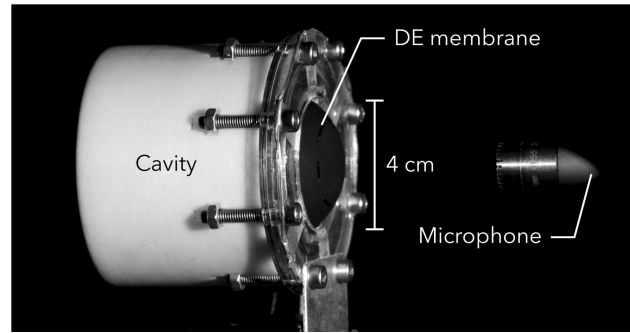axially prestretched by a factor of 1.1, and coated by carbon-black–loaded silicone electrodes applied by pad printing [26]. The membrane is then placed on a closed cavity of 3 cm radius and 5 cm depth and inflated to 1,000 Pa (see Fig. 2). A high-voltage amplifier Trek 609E-6 is used to amplify the audio signal and drive the loudspeaker.

The acoustic transfer functions which are shown in the rest of the article have been measured in an anechoic chamber, whose dimensions are $3 \times 3 \times 3$ m, and which specified down to 120 Hz. The transfer function between the excitation signal and the radiated pressure is computed using the exponential swept-sine method by Farina [27], which yields both the transfer function and an estimate of the harmonic distortion.

1.2 Model of the Inflated DE Loudspeaker

In this section, we present an overview of the modeling procedure described in detail in [14, 15], as this model is at the core of the adaptive filtering algorithm introduced later in section Sec. 2.

1.2.1 Electromechanical Coupling in the DE Membrane

The voltage difference imposed on the membrane's opposite faces induces an electrical field which creates a stress in the membrane material. This electromechanical coupling differs from standard electrodynamic loudspeakers, where the actuation mechanism is based on the Lorentz force. The electromechanical coupling is modeled here by the Maxwell electrostatic pressure which equals [28, 29]

$$\sigma_{Maxwell} = \frac{1}{2}\varepsilon\frac{u^2}{h^2} \,, \tag{1}$$

where u the applied voltage, ε the membrane permittivity, and h the membrane thickness.

It has to be noted that the electrostatic stress is proportional to the voltage squared u^2, which, if not treated properly, would lead to strongly nonlinear transducers. In order to avoid this phenomenon, the loudspeaker is driven by the following voltage [4]:

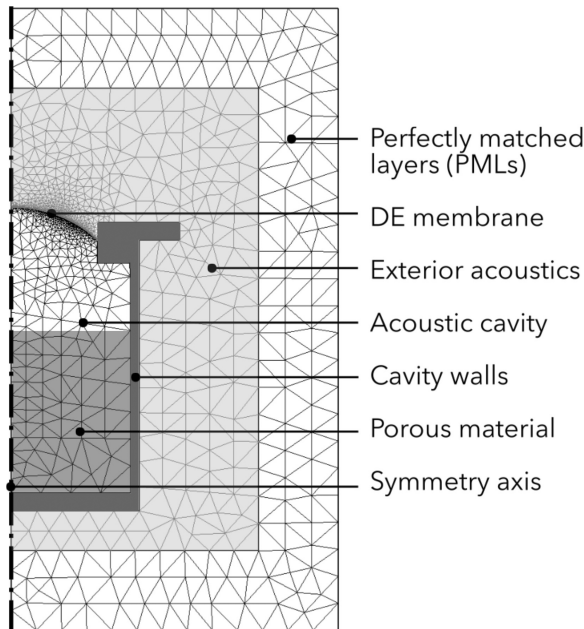$$u(t) = U\sqrt{1 + w(t)} \,, \qquad \text{with } |w| < 1 \,, \tag{2}$$

Fig. 3. Geometry and mesh of the finite element model of the axisymmetric inflated dielectric elastomer (DE) membrane shown in Fig. 2.

where U is a static bias voltage and $w(t)$ the audio signal. This form of the excitation implies that the electrostatic stress is proportional to the signal w. Of course, other sources of nonlinearities may cause distortion, but the quadratic nonlinearity that is inherent to DE devices is cancelled.

1.2.2 Vibroacoustic Coupling

Another characteristic of DE loudspeakers results from the thinness of the membrane, which yields strong added mass effects. It is therefore necessary to take into account the strong coupling between the membrane and acoustics to capture accurately the dynamics and sound radiation of the system. Here, the coupled vibroacoustic problem is written in a monolithic form, by discretizing the fluid and solid domains by finite elements in the open-source software FreeFEM [30] (see Fig. 3). At the exterior boundary of the domain, the Sommerfeld radiation condition must be satisfied. This condition is implemented by perfectly matched layers (PMLs) [31], which are modified to become frequency independent.

The finite element approach results in the description of the full system as a large set of coupled dynamical equations governing the harmonic evolution of the degrees of freedom of the system at the frequency ω of the electrical forcing: $x_{tot}(t) = Re(X_{tot}e^{i\omega t})$. This system is written in the form [1]

$$(-\omega^2 M_{tot} + K_{tot})X_{tot} = F_{tot} , \qquad (3)$$

where M_{tot} and K_{tot} are the total mass and stiffness matrices, which are frequency independent, and $X_{tot} = [Q_i, Q_e, X]^T$ is the complex amplitude of all the degrees of freedom of the system, with x representing the displacement of the DE membrane. We introduced the displacement potentials for interior and exterior acoustics by $Q_i = P_i/\omega^2$ and $Q_e = P_e/\omega^2$, where P_i and P_e are the acoustic pressures inside and outside of the cavity, respectively. This choice of variables in the fluid improves the convergence of the modal truncation presented in [14]. The right hand side F_{tot} is the electrostatic excitation force.

The losses in the membrane are modeled as structural damping [32], and those due to radiation are taken into account by the PMLs. As a result, the system matrices M_{tot} and K_{tot} are complex and include dissipation effects.

1.2.3 Modal Solving

The system Eq. (3) obtained by finite elements is typically very large, with about 10,000 degrees of freedom. Inverting directly the system Eq. (3) to obtain X_{tot} for each frequency is therefore too slow to be used in a real-time application.

To accelerate the resolution, modal methods can be used. In the absence of external forcing ($F_{tot} = 0$), the system Eq. (3) is a linear eigenvalue problem, which can therefore be solved using standard eigenvalue solvers. Consequently, modal expansions of the membrane vibrations X, and of the interior and exterior acoustic pressures P_i and P_e are obtained as follows:

$$X = \sum_n \Psi_n^x \frac{F_n}{\mu_n(\omega_n^2 - \omega^2)} , \qquad (4)$$

$$P_i = \sum_n \Psi_n^i \frac{\omega^2 F_n}{\mu_n(\omega_n^2 - \omega^2)} , \qquad (5)$$

$$P_e = \sum_n \Psi_n^e \frac{\omega^2 F_n}{\mu_n(\omega_n^2 - \omega^2)} , \qquad (6)$$

where ω_n are the eigenfrequencies, F_n the modal forces, μ_n the modal masses, and Ψ_n^x, Ψ_n^i, and Ψ_n^e the parts of the coupled modeshapes containing the structural, interior acoustics, and exterior acoustics degrees of freedom, respectively. This solving method based on a modal approach for exterior problems provides a better insight in the physics of the system than the direct approach consisting of inverting Eq. (3) for all frequencies of interest [33, 34].

The method described above yields the radiated acoustic pressure only in the part of the domain that is meshed (referred to as "exterior acoustics" in Fig. 3). To compute the far-field pressure, we use the Kirchhoff–Helmholtz integral to propagate the near field solution [35].

Once the modal parameters are known (modeshapes, modal force, and eigenfrequencies), a frequency response can be computed very quickly, as only the summation Eq. (6) needs to be performed. The transfer function between the excitation signal w and the acoustic pressure at any point at 1,000 frequency bins can be computed in less than 2 s on a standard computer using the modal method, while it takes about 50 s using the direct inversion of Eq. (3).
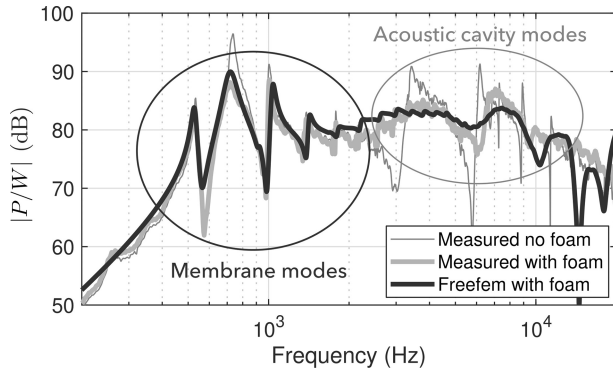
Fig. 4. Transfer function between the pressure p radiated at 1 m on-axis and the excitation signal w, for the dielectric elastomer (DE) loudspeaker inflated to 1000Pa , measured and computed using the multi-physic finite element code in FreeFEM. In the second measurement, the acoustic cavity is filled with porous material (see Fig. 3), which damps out the cavity modes. The peaks at low frequencies are due to the eigenmodes of the membrane and are little affected by the added porous material.

1.3 Validation of the Model

As a first example, a comparison between the results of the model and the experiments is presented. The pressure radiated by the inflated DE loudspeaker is measured on-axis at 1 m and plotted in Fig. 4, together with the results of the model. The model yields an accurate prediction of the radiated sound, from 200 Hz to 10 kHz.

The frequency response in Fig. 4 is very disturbed at low frequencies (between 500 Hz and 2,000 Hz) due to the membrane modes. Above 2 kHz, large peaks and dips due to acoustic resonances of the cavity are observed. Fig. 4 also shows that adding porous material in the cavity helps to damp the acoustic cavity modes but is inefficient at damping the membrane modes.

It is hence possible to regularize the frequency response of this loudspeaker at high frequencies above 2 kHz by the damping approach. To treat the low-frequency range, we propose an adaptive equalization strategy, which uses the computed frequency response to build the filter.

2 ADAPTIVE FILTERING STRATEGY

As mentioned in the introduction, the properties of DE loudspeaker are more likely to evolve in time than those of electrodynamic loudspeakers. The frequencies of the membrane modes which cause the large peaks and dips in Fig. 4 may change, so the inverse filter should follow their evolution.

The principle of the method is to use the previously introduced finite element model to compute the acoustic frequency response of the loudspeaker and use it to derive the equalization filter. The model parameters are then updated using real-time measurements to yield an adapted filter. Because we aim to propose a realistic audio setup, the project will involve only a real-time impedance measurement. This method is simple and nonintrusive, as it doesn't require any added sensor, like a microphone, for example.
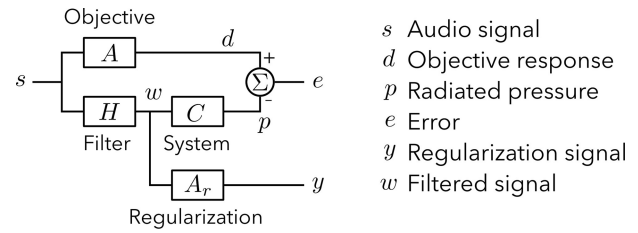

Fig. 5. Block diagram of the system, and definition of the signals. The system transfer function C used to compute the inverse filter is obtained from the model presented in Sec. 2. The objective function A can be arbitrarily chosen, and the guidelines to design the regularization function A_r exist in the literature [36, 24].

Moreover, the adaptation algorithm relies on the following assumption: *when the system parameters evolve, the eigenfrequencies change, but the variations of the mode-shapes, modal damping, and modal forces can be neglected.* Thus, it is sufficient to adapt the eigenfrequencies in the model to obtain an adapted inverse filter.

In this section, the method is described in detail, first by explaining the design of the inverse filter from a given frequency response and then by presenting the adaption procedure.

2.1 Inverse Filter Design

Here, we describe the method proposed by Norcross et al. [24] to design a minimum phase FIR inverse filter from a measured or computed frequency response. Fig. 5 shows the block diagram of the implemented system, as well as the definition of all the implied time signals. We recall that signals are denoted by small letters in the time domain and by capital letters in the frequency domain.

The goal of the following developments is to find the optimal filter H that minimizes the cost function J, built as follows:

$$J(\omega) = \frac{1}{2}E(\omega)E(\omega)^* + \beta Y(\omega)Y(\omega)^* , \qquad (7)$$

where the star * denotes the complex conjugate and β is a regularization parameter introduced to reduce the inverse filter length [17]. Substituting the expressions of $E = (A - HC)S$ and $Y = HA_rS$ in terms of S and minimizing the cost function yields the following optimal expression for the inverse filter H:

$$H(\omega) = \frac{C^*(\omega)A(\omega)}{|C(\omega)|^2 + \beta|A_r(\omega)|^2} . \qquad (8)$$

Norcross et al. show that this filter design problem is equivalent to a system without regularization but with a modified objective function A_{eq}. The optimal filter for the system of Fig. 5 without the regularization is as follows:

$$H(\omega) = \frac{C^*(\omega)A_{eq}(\omega)}{|C(\omega)|^2} . \qquad (9)$$

Equating Eqs. (8) and (9) yields the following:

$$A_{eq}(\omega) = \frac{A(\omega)}{1 + \beta|A_r(\omega)|^2/|C(\omega)|^2} . \qquad (10)$$
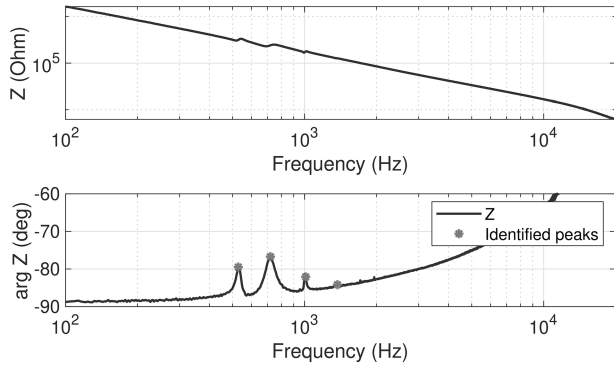
Fig. 6. Impedance Z of the dielectric elastomer (DE) loudspeaker and identified peaks. The peaks correspond to the first four eigenmodes of the membrane, which cause the first peaks in Fig. 4.

If the objective function is only an amplitude term, the phase of the equivalent target function A_{eq} can be chosen arbitrarily and especially minimum phase. To this aim, the phase of $A_{eq}(\omega) = |A_{eq}(\omega)|\exp[i\phi_{eq}(\omega)]$ is set to [24]:

$$\phi_{eq}(\omega) = -\text{imag}\left[\text{Hilbert}\left(\ln\left|A_{eq}(\omega)\right|\right)\right] . \qquad (11)$$

In the following text, we will equalize the loudspeaker only in the frequency band $[\omega_{min} - \omega_{max}]$. We therefore choose $A_r(\omega) = 1$ in $[\omega_{min} - \omega_{max}]$ and $A_r(\omega) = 0$ otherwise. The objective function is set to $A(\omega) = 1$ for ω in$[\omega_{min} - \omega_{max}]$ and $A(\omega) = |C(\omega)|$ otherwise. Outside of $[\omega_{min} - \omega_{max}]$, the filter amplitude is thus $|H(\omega)| = 1$. Further discussions on how to choose the regularization can be found in [24, 36], for example.

2.2 Adaptation Method

In the present study, for demonstration purposes only one parameter (the inflation pressure) will vary during the experiments. The algorithm which is developed here may, however, be used for other changes, like, for example, softening of the elastomer due to temperature changes, as long as the assumption introduced in section 2 remains valid.

Due to electromechanical coupling the impedance of the loudspeaker exhibits peaks at the first eigenfrequencies (see Fig. 6), so it is possible to estimate the frequencies of the first membrane modes by electrical measurements and use them in the model to adapt the equalization filter. The same phenomenon occurs in electrodynamic loudspeakers even though it is caused by a different electromechanical coupling mechanism: the impedance exhibits a peak at the resonance frequency of the system [37].

The adaptation algorithm is described in detail in Fig. 7. First, before the system is launched, the finite element calculation is carried out with standard parameters, which correspond to the reference operational point (around which the system may evolve). The modeshapes, eigenfrequencies, modal damping, and modal forces are computed.

The filtering system operates in parallel: On the one side, the audio real-time loop operates with a frame length of 2^{14} samples, and is implemented using the Matlab Audio Toolbox. This loop reads the audio stream, as well as the
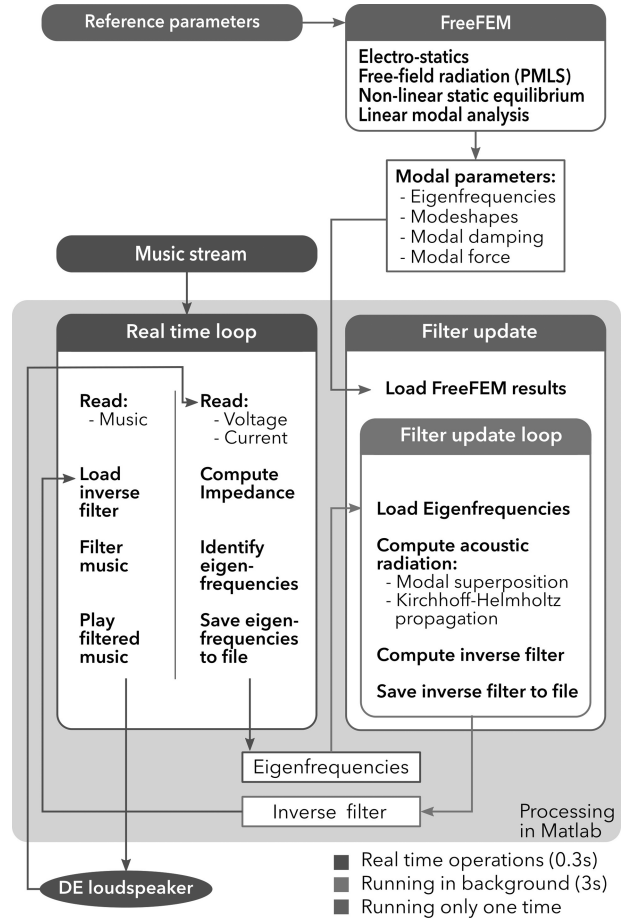

Fig. 7. Adaptive control flowchart. The items on the left-hand side are processed by a real-time loop, based on a frame-length of 2^{14} samples at the sampling frequency $F_s = 44,100$ Hz. The filter update loop takes about 3 s, and is run in parallel of the real-time loop. These two loops communicate by files that are saved on the computer. The operations in the light grey boxes typically take longer time (several minutes) but are only performed one time.

voltage and current flowing through the DE loudspeaker. It loads the latest version of the inverse filter, applies it to the audio stream by a frequency domain convolution, and sends it to the loudspeaker. Simultaneously, the transfer function between the voltage and the current is computed using a frequency-domain averaging method to yield the impedance [32]. The peaks are identified by a peak-picking algorithm to estimate the first four eigenfrequencies of the DE membrane (see Fig. 6). These frequencies are saved in a file on the computer.

A more computationally heavy and non-real-time loop is run in parallel to the real-time loop to take care of the filter update. In this loop, the eigenfrequencies which are identified in real time are uploaded, and inserted in the modal summation Eq. (6). The near field solution is then propagated to the far field using the Kirchhoff–Helmholtz integral as described in Sec. 1 to obtain the transfer function between the excitation signal w and the radiated pressure p on-axis at 1 m. This transfer function is used to compute the inverse filter following the method of Norcross et al., as described in Sec. 2.1. Finally, the inverse filter is saved
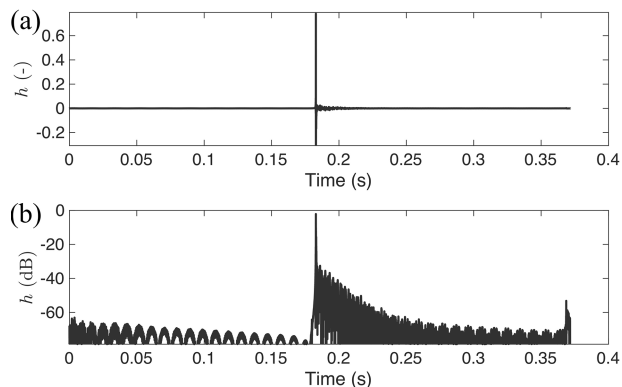
(a)

(b)

Fig. 8. Impulse response of the inverse filter, obtained from the transfer function between the pressure p on-axis at 1 m and the excitation signal s, for an inflation pressure of 1,000 Pa. The inverse filter is designed to be minimum phase, so all the energy of the filter is located after the main impulse. This avoids any preringing effect. (a) Linear scale. (b) Amplitude on logarithmic scale.
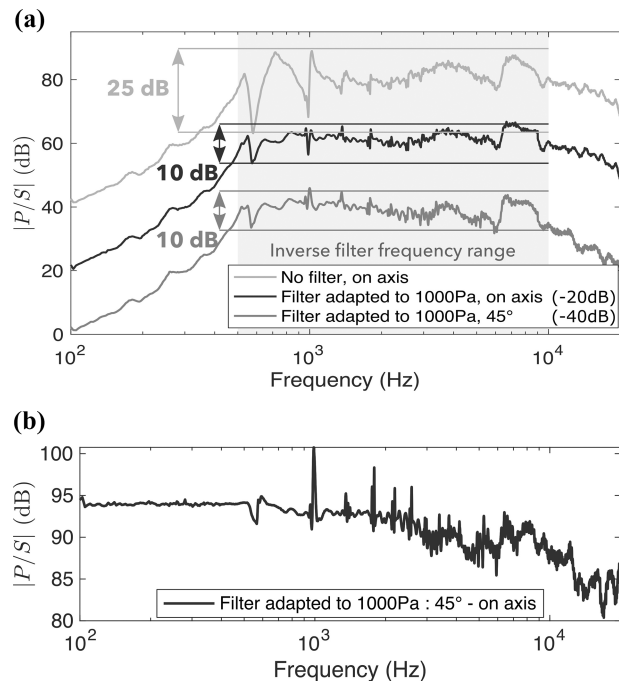

(a)

(b)

Fig. 9. Acoustic frequency response of the dielectric elastomer (DE) loudspeaker inflated to 1,000 Pa, measured at 1 m. The first plot is obtained without inverse filtering and the second and third with a filter computed using a frequency response obtained by a finite element calculation at 1,000 Pa. The second and third plots are shifted 20 and 40 dB downwards to increase readability. (a) Measured frequency response. (b) Difference between the response 45° from axis and the response on-axis.

in a file so that the real-time loop can have access to it. The whole filter update process takes about 3 s. Also, for demonstration purposes, the transfer function between the radiated pressure and the input audio stream is measured in real time to assess the efficiency of the adaptive filtering strategy.

3 RESULTS AND DISCUSSION

In this section, the efficiency of the proposed adaptive filtering strategy is assessed in terms of flatness of the frequency response. Other performance criteria could have been considered, like (for example) the phase of the transfer function between the excitation and the radiated pressure, but as we chose to only perform an amplitude equalization, we focus on the amplitude of the frequency response in this first approach.

3.1 Efficiency of the Inverse Filter

First, the efficiency of the inverse filter is assessed, independently of the adaptation algorithm. The inflation pressure is fixed, so the eigenfrequencies of the membrane do not change during the measurement. The first four eigenfrequencies are estimated from the impedance and used to compute the filter. The filter is thus adapted to the actual state of the loudspeaker. The filter is designed to flatten the frequency response only in the range from 500 to 10,000 Hz to avoid overloading the loudspeaker below its cut-off frequency and to avoid generating spurious peaks at high frequencies due to a mismatch between the measured and the computed transfer function (see Fig. 4).

The inverse filter impulse response h (from Eq. (8)) is plotted in Fig. 8. All the energy of the filter is located after the main peak, showing that it is minimum phase and that no preringing effect will occur [24].

The transfer function between the radiated pressure p on-axis at 1 m and the excitation signal s is measured and

plotted in Fig. 9(a), with and without applying the inverse filter H. Without filter, there are large peaks and dips around 800 Hz, which are caused by the first membrane modes, as explained in Sec. 1. There is a difference in amplitude between the dips and peaks by more than 25 dB. When the filter is applied, this amplitude difference is reduced to 10 dB. Also, at higher frequencies, around 5 kHz, the filtered frequency response is flatter than the original one. The efficiency of the filter is limited by the accuracy of the finite element model; an even flatter frequency could potentially be obtained by a better prediction of the modal loss factors, for example.

A common limitation of equalization based on a single microphone position (for example, here on-axis at 1 m) is that the equalization may deteriorate the response at other positions, typically off-axis. However, in the present case, the loudspeaker is acoustically compact at the frequencies of the first membrane modes (around 1 kHz) and thus has an omnidirectional directivity pattern [14] (see Fig. 9(b)). Therefore, the improvement observed on-axis should be observed off-axis as well. This is demonstrated in Fig. 9(a), in which the radiation is measured at 1 m at 45° from the axis. Fig. 9(a) shows that the improvement obtained by inverse filtering on-axis is also obtained off-axis. The only difference between on- and off-axis responses is the roll-off at high frequencies, which is steeper off-axis, as seen in Fig. 9(b), as the loudspeaker radiates more on-axis than off-axis at high frequencies.
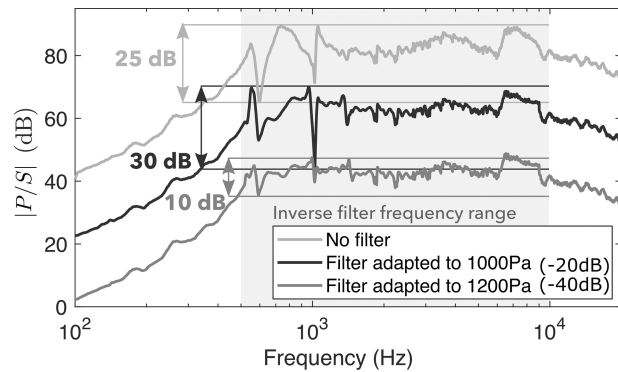
Fig. 10. Acoustic frequency response of the DE loudspeaker inflated to 1,200 Pa, measured at 1 m on-axis. The top curve is obtained without inverse filtering and the middle curve with a filter that is adapted to an inflation pressure of 1,000 Pa. The bottom curve is obtained with an adapted filter, in which the frequencies of the first four modes have been adjusted to match the peaks in the impedance. The middle curve is shifted 20 dB and the bottom one 40 dB downwards to increase readability.

Fig. 11. Video demonstrating the adaptive filtering in real time, with white noise and music [(https://hal.archives-ouvertes.fr/hal-03221229 [38])].

The efficiency of the filter has been demonstrated when the filter is derived from a frequency response which has been computed at the correct inflation pressure. The adaptation of the filter to an evolution of the system will now be investigated.

3.2 Adaptation of the Filter

Only one finite element calculation is performed, for an inflation pressure of 1,000 Pa, and used to compute all the inverse filters, which will be used in the following. The DE loudspeaker is now inflated to 1,200 Pa. Three transfer functions are measured without filter, with the original filter (which is adapted to the reference pressure of 1,000 Pa), and with the inverse filter computed in the filter update loop of Fig. 7, once the frequencies of the first four membrane modes have been adjusted to the actual measured frequencies at 1,200 Pa. The results are plotted in Fig. 10.

Fig. 10 shows that when the filter which is adapted to 1,000 Pa is used, large peaks and dips are observed in the frequency response. This occurs because the membrane eigenfrequencies have increased when the inflation pressure has been raised, so the peaks and dips of the filter are no longer located at the correct frequencies. As a consequence, the filter does not help improving the frequency response and may even have a negative effect. This highlights that it is necessary to update the inverse filter.

Once the frequencies of the first modes are updated in the filter calculation, the frequency response is improved, and the difference in magnitude between the peaks and the dips drops below 10 dB. This demonstrates that the proposed adaptive filtering strategy succeeds in following the system's dynamics and helps to improve the acoustic behavior of the loudspeaker.

3.3 Testing in Operational Conditions

The plots that are shown in the present article have been obtained by using a frequency sweep as the excitation sig-
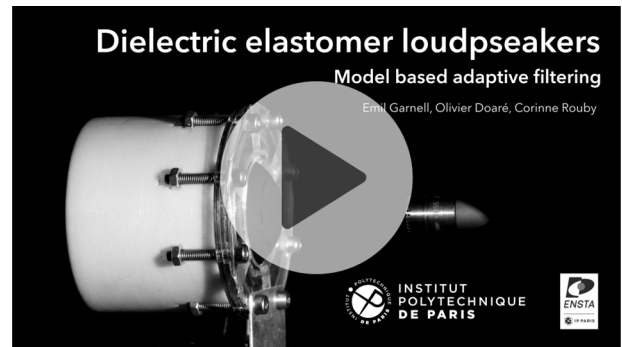
nal, but they can be obtained in a similar manner by using the music signal. The impedance is estimated in real time but may sometimes be erroneous when there is no excitation signal (for example, between two songs). To increase the robustness of the method, a stability criterion is added in the peak detection in the impedance to obtain the membrane modes: An identified eigenfrequency is considered valid only if it has been identified in 10 consecutive frames. Finally, the filter converges to the optimal solution about 3 s after a change of the system's parameters, such as the inflation pressure, for example. To visualize and listen to the effect of inverse filtering and filter adaptation for realistic signals, the reader is encouraged to watch the video in Fig. 11 [38] in which the whole system is demonstrated in real time.

3.4 Limitations

The proposed adaptive filtering strategy relies on the assumption that the modeshapes, the modal damping, and the modal forces do not change much when the system evolve. While this is true for small evolutions of the system around a reference state (for example, pressure variations of a few hundreds pascals), it no longer holds for large changes in the system's parameters. As a consequence, the adaption of the filter would not work for pressures that are far away from the reference pressure at which the finite element calculation was performed. For the prototype studied in this article, the employed adaptation strategy allows to maintain the sound pressure level variations under 10 dB for static pressure variations smaller than 40%.

Also, in this study, we considered only amplitude equalization, but nothing prevents the filter from being designed to perform phase equalization as well. Previous research on modeling of DE loudspeakers demonstrated that the finite element model that is used in this study also predicts accurately the phase of the transfer function between the radiated pressure and the audio signal [14]. It should also be possible to use an IIR inverse filter to decrease the latency of the filtering algorithm.

Finally, the whole study is limited to linear analysis: The finite element model computes only linear dynamics for now, and the whole inverse filtering method is intrinsically
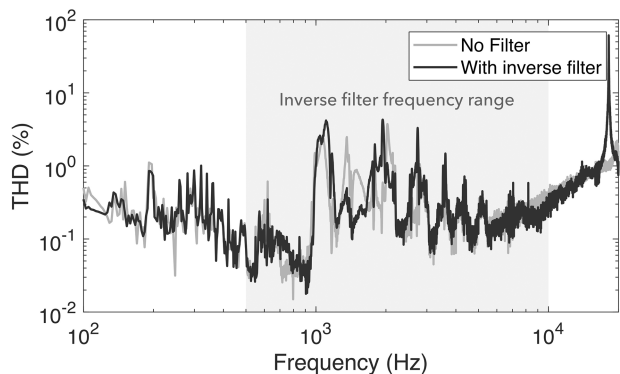
Fig. 12. Total harmonic distortion of the pressure at 1 m on-axis, with and without the inverse filter.

linear as well. Thus, the total harmonic distortion (THD) is not improved by the proposed filtering method, as seen in Fig. 12. The results of Fig. 12 are obtained with a bias voltage $U = 2,000$ V and $|w| = 0.05$, which corresponds to a relatively low level (about 60 dB SPL at 1 m). For larger values of $|w|$, the THD is larger, and this remains a problem to be solved.

4 CONCLUSION

In this article, we have addressed one of the limitations of DE loudspeakers by implementing an adaptive filtering method that improves the spectral balance. We demonstrated that accurate modeling of DE devices especially at high frequencies opens new solutions to optimize their design an overcome some of their limitations.

Many challenges still have to be addressed before DE loudspeakers can reach to the market, the main ones being reducing the driving voltage from kilovolts to hundreds of volts, understanding better the failure mechanisms of DE actuators to improve their lifetime, and finding solutions to reduce harmonic distortion that for now remains higher than in electrodynamic loudspeakers. We believe that improved modeling of the dynamics of DE devices opens new challenges and may trigger further improvements.

5 ACKNOWLEDGMENTS

6 REFERENCES

[1] R. Pelrine, R. Kornbluh, Q. Pei, and J. Joseph, "High-Speed Electrically Actuated Elastomers With Strain Greater Than 100%," *Science*, vol. 287, no. 5454, pp. 836–839 (2000 Feb.).

[2] J. Huang, T. Li, C. Chiang Foo, J. Zhu, D. R. Clarke, and Z. Suo, "Giant, Voltage-Actuated Deformation of a Dielectric Elastomer Under Dead Load," *Appl. Phys. Lett.*, vol. 100, no. 4, paper 041911 (2012 Jan.).

[3] R. Heydt, R. Kornbluh, R. Pelrine, and V. Mason, "Design and Performance of an Electrostrictive Polymer-Film Acoustic Actuator," *J. Sound Vib.*, vol. 215, no. 2, pp. 297–311 (1998 Aug.).

[4] R. Heydt, R. Pelrine, J. Joseph, J. Eckerle, and R. Kornbluh, "Acoustical Performance of an Electrostrictive Polymer Film Loudspeaker," *J. Acoust. Soc. Am.*, vol. 107, no. 2, pp. 833–839 (2000).

[5] R. Heydt, R. Pelrine, R. Kornbluh, N. Bonwit, and J. Eckerle, "Compliant Electroactive Polymer Transducers for Sonic Applications," U.S. Patent No. 7,608,98 (2009 Oct.).

[6] R. Pelrine, R. Kornbluh, and J. Eckerle, "Elastomeric Dielectric Polymer Film Sonic Actuator," U.S. Patent No. 6,343,129 (2002 Jan.).

[7] N. Hosoya, S. Baba, and S. Maeda, "Hemispherical Breathing Mode Speaker Using a Dielectric Elastomer Actuator," *J. Acoust. Soc. Am.*, vol. 138, no. 4, pp. EL424–EL428 (2015 Oct.).

[8] N. Hosoya, H. Masuda, and S. Maeda, "Balloon Dielectric Elastomer Actuator Speaker," *Appl. Acoust.*, vol. 148, pp. 238–245 (2019 May).

[9] T. Sugimoto, A. Ando, K. Ono, Y. Morita, K. Hosoda, D. Ishii, et al., "A Lightweight Push–Pull Acoustic Transducer Composed of a Pair of Dielectric Elastomer Films," *J. Acoust. Soc. Am.*, vol. 134, no. 5, pp. EL432–EL437 (2013 Oct.).

[10] E. Rustighi, W. Kaal, S. Herold, and A. Kubbara, "Experimental Characterisation of a Flat Dielectric Elastomer Loudspeaker," *Actuators*, vol. 7, no. 2, paper 28 (2018 Jun.).

[11] J. W. Fox and N. C. Goulbourne, "Electric Field-Induced Surface Transformations and Experimental Dynamic Characteristics of Dielectric Elastomer Membranes," *J. Mech. Phys. Solids*, vol. 57, no. 8, pp. 1417–1435 (2009 Aug.).

[12] J. Zhu, S. Cai, and Z. Suo, "Resonant Behavior of a Membrane of a Dielectric Elastomer," *Int. J. Solids Struct.*, vol. 47, no. 24, pp. 3254–3262 (2010 Dec.).

[13] P. Dubois, S. Rosset, M. Niklaus, M. Dadras, and H. Shea, "Voltage Control of the Resonance Frequency of Dielectric Electroactive Polymer (DEAP) Membranes," *J. Microelectromech. Syst.*, vol. 17, no. 5, pp. 1072–1081 (2008 Oct.).

[14] E. Garnell, O. Doaré, and C. Rouby, "Coupled Vibro-Acoustic Modeling of a Dielectric Elastomer Loudspeaker," *J. Acoust. Soc. Am.*, vol. 147, no. 3, pp. 1812–1821 (2020 Mar.).

[15] E. Garnell, C. Rouby, and O. Doaré, "Dynamics and Sound Radiation of a Dielectric Elastomer Membrane," *J. Sound Vib.*, vol. 459, paper 114836 (2019 Oct.).

[16] M. Karjalainen, V. Ikonen, P. Antsalo, P. Maijala, L. Savioja, A. Suutala, et al., "Comparison of Numerical Simulation Models and Measured Low-Frequency Behavior of Loudspeaker Enclosures," *J. Au-*

dio Eng. Soc., vol. 49, no. 12, pp. 1148–1166 (2001 Dec.).

[17] H. Tokuno, O. Kirkeby, P. A. Nelson, and H. Hamada, "Inverse Filter of Sound Reproduction Systems Using Regularization," *IEICE Trans. Fundam. Electron. Commun. Comput. Sci.*, vol. E80-A, no. 5, pp. 809–820 (1997).

[18] G. Ramos and J. J. López, "Filter Design Method for Loudspeaker Equalization Based on IIR Parametric Filters," *J. Audio Eng. Soc.*, vol. 54, no. 12, pp. 1162–1178 (2006 Dec.).

[19] A. Gabrielsson, B. Lindström, and O. Till, "Loudspeaker Frequency Response and Perceived Sound Quality," *J. Acoust. Soc. Am.*, vol. 90, no. 2, pp. 707–719 (1991 Aug.).

[20] R. J. Oliver and J.-M. Jot, "Efficient Multi-Band Digital Audio Graphic Equalizer with Accurate Frequency Response Control," presented at the *139th Convention of the Audio Engineering Society* (2015 Oct.), paper 9406.

[21] O. Doaré, G. Kergourlay, and C. Sambuc, "Design of a Circular Clamped Plate Excited by a Voice Coil and Piezoelectric Patches Used as a Loudspeaker," *J. Vib. Acoust.*, vol. 135, no. 5, paper 051025 (2013 Jun.).

[22] M. Karjalainen, E. Piirilä, A. Järvinen, and J. Huopaniemi, "Comparison of Loudspeaker Equalization Methods Based on DSP Techniques," *J. Audio Eng. Soc*, vol. 47, no. 1/2, pp. 14–31 (1999 Feb.).

[23] L. D. Fielder, "Analysis of Traditional and Reverberation-Reducing Methods of Room Equalization," *J. Audio Eng. Soc.*, vol. 51, no. 1/2, pp. 3–26 (2003 Feb.).

[24] S. G. Norcross, M. Bouchard, and G. A. Soulodre, "Inverse Filtering Design Using a Minimal- Phase Target Function from Regularization," presented at the *121st Convention of the Audio Engineering Society* (2006 Oct.), paper 6929.

[25] F. Klug, C. Endl, S. Solano-Arana, and H. F. Schlaak, "Design, Fabrication, and Customized Driving of Dielectric Loudspeaker Arrays," in *Proceedings of SPIE*

10966, Electroactive Polymer Actuators and Devices (EA-PAD) XXI, paper 109662I (Denver, CO) (2019 Mar.).

[26] S. Rosset, O. A. Araromi, S. Schlatter, and H. R. Shea, "Fabrication Process of Silicone-based Dielectric Elastomer Actuators," *J. Visualized Exp.*, vol. 108, paper 53423 (2016 Feb.).

[27] A. Farina, "Simultaneous Measurement of Impulse Response and Distortion with a Swept-Sine Technique," presented at the *108th Convention of the Audio Engineering Society* (2000 Feb.), paper 5093.

[28] A. Kovetz, *Electromagnetic Theory* (Oxford University Press, Oxford, UK, 2000).

[29] Z. Suo, "Theory of Dielectric Elastomers," *Acta Mech. Solida Sin.*, vol. 23, no. 6, pp. 549–578 (2010 Dec.).

[30] F. Hecht, "New Development in Freefem++," *J. Numer. Math.*, vol. 20, no. 3-4, pp. 251–265 (2012).

[31] J.-P. Berenger, "A Perfectly Matched Layer for the Absorption of Alectromagnetic Waves," *J. Comput. Phys.*, vol. 114, no.2, pp. 185–200 (1994 Oct.).

[32] D. J. Ewins, *Modal Testing: Theory and Practice*, vol. 15 (Research Studies Press, Letchworth, UK, 1984).

[33] S. Marburg, "Normal Modes in External Acoustics. Part I: Investigation of the One-Dimensional Duct Problem," *Acta Acust. united Acust.*, vol. 91, no. 6, pp. 1063–1078 (2005 Nov.).

[34] P. Lalanne, W. Yan, K. Vynck, C. Sauvan, and J.-P. Hugonin, "Light Interaction with Photonic and Plasmonic Resonances," *Laser Photonics Rev.*, vol. 12, no. 5, paper 1700113 (2018 May).

[35] L. L. Beranek and T. J. Mellow, *Acoustics: Sound Fields and Transducers* (Academic Press, Oxford, UK, 2012).

[36] O. Kirkeby and P. A. Nelson, "Digital Filter Design for Inversion Problems in Sound Reproduction," *J. Audio Eng. Soc.*, vol. 47, no. 7/8, pp. 583–595 (1999 Jul.).

[37] N. Thiele, "Loudspeakers in Vented Boxes: Part 1," *J. Audio Eng. Soc.*, vol. 19, no. 5, pp. 382–392 (1971 May).

[38] E. Garnell, O. Doaré, and C. Rouby, "Model Based Adaptive Filtering of a Dielectric Elastomer Loudspeaker," https://hal.archives-ouvertes.fr/hal-03221229 (accessed May 13, 2021).

THE AUTHORS

Emil Garnell defended his Ph.D. thesis on the modeling and optimization of dielectric elastomer loudspeakers in 2020 at ENSTA Paris, France, and is now working as a signal processing research engineer at Devialet, Paris, France.

•

Olivier Doaré is a Professor at ENSTA Paris, France, since 2003. The main research field he has been involved in concerns the coupling between active structures and fluids and, in particular, the modeling, simulation, and optimization of electroacoustic transducers.

•

Corinne Rouby is an Assistant Professor at ENSTA Paris, France, since 2010. Her research interests are in the field of coupled systems, such as dielectric elasomer membranes, magnetic structures, and liquid-filled cracks.